

Introduction: The quantity and distribution of lunar volatiles in polar cold traps may be a source of volatiles for In Situ Resource Utilization (ISRU) space resource architectures. Current research focuses on lunar volatiles' presence and spatial extent [1, 2]. A body of work also examines the depth to the top of volatile stability zones [3, 4]. However, research is needed to define the depth to the base of volatile stability zones, changes of stability zone shape with crater infill, and potential remobilization of volatiles in regolith.

The water ice stability zone exists where regolith surface temperatures are below ~ 110 K [5], or regolith subsurface temperatures are below ~ 145 K [4, 6]. Volatiles may exist in lunar regolith as discrete grains of ice, adsorbed onto regolith grains, or as discrete layers of ice [7]. Large impacts or volcanic events may have formed relatively ice-rich layers similar to those observed in cold traps near Mercury's poles [8]. Over time, gardening processes will mix, bury, and expose the ice and icy regolith mixtures. Erosional processes will remove volatiles at the surface [9]. Icy regolith mixtures may also be buried and protected from gardening by blanketing impact ejecta layers [10].

This work explores the hypothesis that volatiles may experience subsurface temperatures that could sublimate ice from the base of cold traps. The temperature conditions may exist to redeposit volatiles in other parts of subsurface cold traps. We also explore a potential positive feedback in which increased ice content improves the thermal conductivity of icy regolith mixtures, thickening volatile stability zones [4]. The remobilization and positive feedback in thermal conductivity may result in more ice at shallower depths and closer to the edges of cold traps than simple volatile and regolith depositional models would imply.

Methods: Here, we calculate two-dimensional (2D) thermal models of regolith and icy regolith mixtures to define modified shapes of volatile stability zones around cold traps. We use the finite element solver in the Python Library for Inversion and Modeling in Geophysics (pyGIMLi) [11]; thermophysical properties of lunar regolith, megaregolith, and water ice along with a range of boundary conditions. We develop synthetic crater profiles, modify them based on topographic diffusion rates, and examine the thermal effects of infill [12]. The heat equation describes how temperature varies in materials [13]. The thermal conductivity varies with composition, density, and temperature. Upper boundary conditions for the model depend on solar energy input and infrared emission to space. We choose an upper boundary condition for the

model outside the cold trap of 160 K, which is the average temperature at 1 m depth for latitudes of ~ 75 degrees [14]. The upper boundary condition inside the cold trap is 110 K [5]. The lower boundary condition is dependent on the subsurface heat flux from the mantle, crustal radioactive sources [13, 15], and the blanketing effects of megaregolith [16]. The regolith thermal conductivity is $0.023 \text{ W m}^{-1} \text{ K}^{-1}$ [18], and megaregolith thermal conductivity is $0.2 \text{ W m}^{-1} \text{ K}^{-1}$ [16]. The heat flux is $.018 \text{ W m}^{-2}$ [15]. We calculated a thermal gradient of 0.09 K/m for the lower boundary condition from the heat flux and the mega regolith thermal conductivity and making an assumption of linearity in the model space. The low-temperature regolith heat capacity function is from [19]. The regolith density with depth function is from [13, 20]. Water ice's thermal conductivity is $5.5 \text{ W m}^{-1} \text{ K}^{-1}$ at 110 K, and the density is 932 kg m^{-3} [21].

Results: We model a lunar crater with a 1 km diameter and calculate 2D temperature profiles (Figures 1-3). Most of the model space has properties consistent with a megaregolith layer that extends from the base of surficial regolith at ~ 5 -20 meters to 2-3 kilometers below the surface [17]. For clarity, the surficial regolith of ~ 10 meters thick is removed from Figures 1-3.

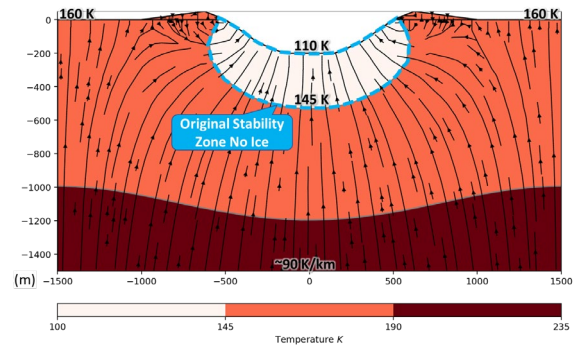


Figure 1. A 2D thermal model of a 1 km diameter crater containing a cold trap. The ice trapping zone is between the 110 K and 145 K temperature isotherms (dashed blue line).

The initial model is a 3 Ga old impact crater shortly after reaching thermal equilibrium. It has a thick volatile stability zone (Figure 1). The crater model is filled with regolith to a thickness consistent with topographic diffusion for three billion years. The filled crater is $\sim 52\%$ of its original depth [12]. The low thermal conductivity regolith infill acts as a blanket to elevate temperatures below the crater. The new base of stability is at or above the original surface of the crater (Figure 2).

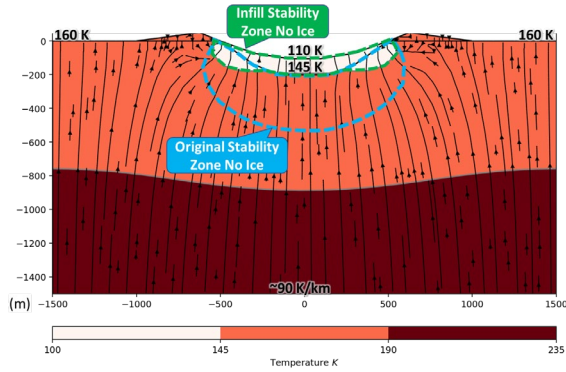


Figure 2. A model with regolith infill that is ice-free or has a low weight percent ice. The new stability zone shows thinning in the middle and less thinning at the edges of the crater (dashed green line).

If low-weight percent ice exists in the regolith fill, it could be sublimated from the base of the fill zone. The cold trapping temperature conditions exist to redeposit the volatile molecules at shallower depths or closer to the edges of the cold trap.

If the crater model contains a layer of relatively pure ice, the base of stability is deeper (Figure 3). The modeled ice layer could represent a Mercury-like layer of ice that formed relatively quickly following a large volatile-rich impact [7, 8, 22]. This scenario requires an ejecta cover following ice deposition to reduce gardening and erosion. The modeled base of stability also stays below the original crater floor if there are 10s of weight percent high thermal conductivity ice mixed with the regolith fill.

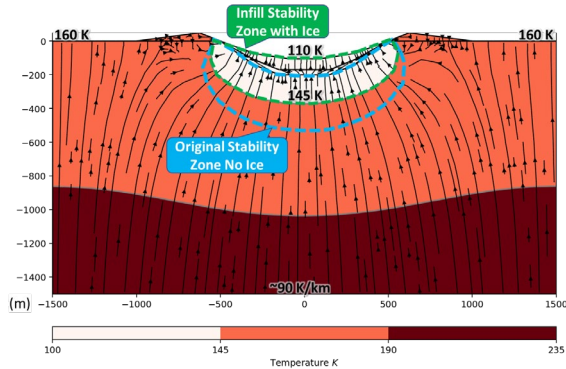


Figure 3. Model of a buried layer of old (~3 Ga) relatively pure ice deposited on the original crater floor.

The ice layer has a high thermal conductivity compared to regolith. This partially compensates for the blanketing effect of regolith infill. This model run indicates a thick layer of ice would enhance its thermal stability by keeping the 145 K isotherm below the original crater floor and the base of the ice layer.

Discussion: The model results support the hypothesis that a low-weight percent icy regolith mixture may sublimate at the base of the stability zone in craters

that are degraded enough to have significant infill. The models indicate that the base of the stability zone may become shallower than the original crater surface creating the potential for volatile remobilization.

Icy regolith mixtures have a higher thermal conductivity than dry regolith but lower than pure ice. Linking the potential remobilization of volatiles from the base of a stability zone with the observation that icy mixtures have a higher thermal conductivity creates scenarios where icy regolith will wick away internal heat more quickly to the surface of cold traps where it will radiate to space. This will depress the depth to the base of the volatile stability zone. This positive feedback may create a reverse "accommodation space" in porous regolith as ice content increases. This could allow pore-filling ice to build down to the limits of regolith porosity and the intergranular volatile migration paths.

Conclusion: This work examines a hypothesis for subsurface volatile remobilization and potential positive feedback with ice concentration that may decrease the depth and increase the thickness of ice stability zones around lunar cold traps. More accurate measurements of both regolith and megaregolith thermophysical properties are critical for understanding and accurately modeling the location and concentration of volatiles in the lunar subsurface.

References: [1] Li, S., et al. (2018), *Proc Natl Acad Sci USA*, 115, 8907–8912. [2] Hayne, P. O., et al. (2015), *Icarus*, 255, 58–69. [3] Schorghofer, N., and Williams, J.-P., (2020), *Planet. Sci. J.*, 1, 54. [4] Siegler, M. A., et al. (2011), *JGR: Planets*, 116. [5] Zhang, J. A., and Paige, D. A., (2009), *GRL*, 36, 5. [6] Schorghofer, N., and Aharonson, O., (2014), *ApJ*, 788, 169. [7] Cannon, K. M., et al. (2020), *GRL*, 47. [8] Ernst, C. M., et al. (2018), *JGR: Planets*, 123, 2628–2646. [9] Farrell, W. M., et al. (2019), *GRL*, 46, 8680–8688. [10] McGetchin, T. R., et al. (1973), *EPSL*, 20, 226–236. [11] Rücker, C., et al. (2017), *Computers & Geosciences*, 109, 106–123. [12] Fassett, C. I., and Thomson, B. J., (2014), *JGR: Planets*, 119, 2255–2271. [13] Hayne, P. O., et al. (2017), *JGR: Planets*, 122, 2371–2400. [14] Martinez, A., and Siegler, M. A., (2021), *JGR: Planets*, 126. [15] Langseth, M. G., et al. (1976), *Geochim. Cosmochim. Acta*. [16] Warren, P. H., and Rasmussen, K. L., (1987), *JGR: Solid Earth*, 92, 3453–3465. [17] Bills, B. G., and Ferrari, A. J., (1977), *JGR* (1896–1977), 82, 1306–1314. [18] Keihm, S. J., and Langseth, M. G., (1975), *Science*, 187, 64–66. [19] Woods-Robinson, R., et al. (2019), *JGR: Planets*, 124, 1989–2011. [20] Heiken, G. H., et al. (1991), Cambridge University Press. [21] Carnahan, E., et al. (2021), *EPSL*, 563, 116886. [22] Rubanenko, L., et al. (2019), *Nat. Geosci.*, 12, 597–601.